Rare Metal Materials and Engineering
Volume 52, Issue 6, June 2023
Available online at www.rmme.ac.cn

Science Press

Cite this article as: Wang Shuyi, Sun Meiqi, Zhang Song, et al. Microstructure and Properties of a Ferromagnetic Damping Alloy Fabricated by Spark Plasma Sintering[J]. Rare Metal Materials and Engineering, 2023, 52(06): 2063-2067.

ARTICLE

Microstructure and Properties of a Ferromagnetic Damping Alloy Fabricated by Spark Plasma Sintering

Wang Shuyi, Sun Meiqi, Zhang Song, Xu Yonggang

Key Laboratory of Advanced Technologies of Materials, Ministry of Education, School of Materials Science and Engineering, Southwest Jiaotong University, Chengdu 610031, China

Abstract: A Fe-16Cr-2.5Mo (wt%) damping alloy was prepared by spark plasma sintering (referred to SPS alloy) and vacuum induction melting followed by forging and annealing (referred to VIMFA alloy). The comparative study on microstructure, magnetic performance, damping capacity and mechanical property of SPS and VIMFA alloys was conducted. Results show that the relatively high compactness of SPS alloy is obtained. The dissolution of Cr and Mo in α-Fe solid solution is obviously promoted and the homogeneity of microstructure of SPS alloy is dramatically ameliorated with increase in sintering temperature and extension in holding time. SPS alloys exhibit relatively lower saturation magnetization but higher coercivity than VIMFA ones. There is still favorable damping capacity for SPS alloys despite it is lower than that of VIMFA one. Furthermore, the damping capacity of SPS alloy slightly rises with increase in sintering temperature and extension in holding time. The SPS alloys possess evidently higher compression strength than VIMFA ones. Also, the compression strength of SPS alloy rises with increase in sintering temperature.

Key words: Fe-Cr based damping alloy; spark plasma sintering; magnetic performance; damping capacity; mechanical properties

As a ferromagnetic damping material, the damping capacity of Fe-Cr based alloy is mainly achieved by the magnetic-mechanical hysteresis damping mechanism. When the external alternating stresses are applied to the alloy, the vibration energy suffered will be converted into heat energy to dissipate through the irreversible movement of the magnetic domain wall in it[1]. Fe-Cr based damping alloys are extremely promising in many fields because of their excellent damping capacity and favorable mechanical properties [2–3].

Conventional preparation of Fe-Cr based damping alloy requires a relatively complex process, i. e. firstly vacuum induction melting, and then forging followed by annealing (referred to VIMFA) [4–5]. The powder metallurgy technology such as hot pressing sintering (HPS) and spark plasma sintering (SPS), has been considered as a favorable method to prepare the alloys possessing homogeneous compositions, fine grains and excellent properties[6]. Moreover, this technology is especially suitable for directly preparing some complex and precise components that can satisfy the engineering requirement[7]. However, the relevant researches regarding the effects of preparation methods on the microstructure and properties of Fe-Cr based damping alloys have hardly been involved before. As a kind of rapid prototyping method of powder metallurgy, the SPS technology is more energy-efficient and environmentally friendly[8], so it was employed to prepare Fe-Cr based damping alloys in this work.

It has been reported that adding appropriate Mo into the Fe-Cr alloy can improve its mechanical properties while maintaining high damping capacity of the alloy[2,9–11]. Combined with our previous studies, a Fe-Cr based damping alloy with a nominal composition of Fe-16Cr-2.5Mo (wt%) has been selected and fabricated by SPS technology. For comparison, this alloy was also prepared by the conventional VIMFA method. The microstructure, magnetic performance, damping capacity and mechanical properties of Fe-Cr based alloys fabricated by SPS and VIMFA were researched comparatively.

1 Experiment

The mixture of pure elemental powders with a nominal

Received date: December 16, 2022
Foundation item: National Natural Science Foundation of China (51701167); Natural Science Foundation of Sichuan Province (2023NSFSC0403)
Corresponding author: Zhang Song, Ph. D., Associate Professor, School of Materials Science and Engineering, Southwest Jiaotong University, Chengdu 610031, P. R. China, Tel: 0086-28-87600712, E-mail: songzhang@home.swjtu.edu.cn

composition of Fe-16Cr-2.5Mo (wt%) was ball-milled at a rotating speed of 330 r/min for 2 h and the ball-to-powder mass ratio was 3: 1. The spark plasma sintering of powder mixture was performed in a vacuum SPS system (LABOX™-350). The SPS samples were firstly heated to target temperature of 900 °C or 1000 °C and then held for 20 or 30 min (referred to SPS900-20, SPS1000-20 and SPS1000-30). Also, a pressure of 30 MPa was applied during SPS process. The alloy with the same composition was fabricated by VIMFA method, specifically vacuum induction melting followed by forging at 1100 °C and annealing at 1000 °C for 30 min.

The samples for microstructural analysis with a size of 8 mm×8 mm×8 mm were cut by electro-discharge machining. The constituent phases of samples were identified by X-ray diffraction (XRD, Panalytical X'Pert Pro, Cu Kα). The microstructure of samples was observed by scanning electron microscopy (SEM, QUANTA FEG 250) using backscattered electron (BSE) imaging, and optical metallographic microscopy (OM, Olympus CX21). The chemical compositions of constituent phases were determined by energy dispersive spectroscopy (EDS, Inca X-sight). The quantitative analysis of microstructure was carried out using Image-Pro Plus 6.0 imaging analysis software.

The magnetization curve and hysteresis loop of samples with a size of 2 mm×2 mm×2 mm were achieved using a vibrating sample magnetometer (VSM, LakeShore 7404). The damping capacity of samples with a size of 1.5 mm×1.5 mm×30 mm was examined in an internal friction instrument using inverted torsion pendulum mode. The variation of damping capacity with strain amplitude was obtained at room temperature with a frequency of 1 Hz. The compressive property of the cylindrical samples with 9 mm in height and 6 mm in diameter was measured by a compression test device (LEGEND 2367) at room temperature with a strain rate of 0.005 s^{-1}.

2 Results and Discussion

2.1 Microstructure of Fe-Cr-Mo alloys

Fig.1 and Fig.2 show the BSE images and XRD patterns of SPS and VIMFA alloys, respectively, and Table 1 presents the chemical compositions of their constituent phases. It can be seen that the microstructures of the alloys obviously change with increase in sintering temperature and extension in holding time. Combined with BSE, XRD and EDS analysis results, the microstructure of SPS900-20 alloy is mainly composed of gray Cr-rich α-Fe, light gray Cr-poor α-Fe, dark Cr and white Mo particles (Fig. 1, Fig. 2, and Table 1). It should be noted that the pure Fe, Cr and Mo elements all have bcc structure at room temperature, and the former two elements have relatively close lattice parameters, about 0.2863 and 0.2884 nm, respectively, which are lower than that of the latter one (0.3147 nm). Meanwhile, considering the relatively small amounts of Cr and especially Mo phases, no obvious diffraction peak of them can be detected in XRD patterns of the alloys (Fig. 2). The microstructure of SPS1000-20 alloy consists primarily of gray Cr-rich α-Fe and light gray Cr-poor α-Fe phases (Fig. 1, Fig. 2, and Table 1). It is indicated that with increasing the sintering temperature from 900 to 1000 °C, Cr and Mo elements almost dissolve into α-Fe solid solution. Moreover, the area fraction of Cr-poor α-Fe phase deceases with increase in sintering temperature (about 39.7% and 10.5% in SPS900-20 and SPS1000-20 alloys, respectively). In contrast, the microstructures of both SPS1000-30 and VIMFA alloys comprise relatively homogeneous α-Fe solid solution (Fig. 1, Fig. 2, and Table 1). It is suggested that the microstructural homogeneity can be achieved by

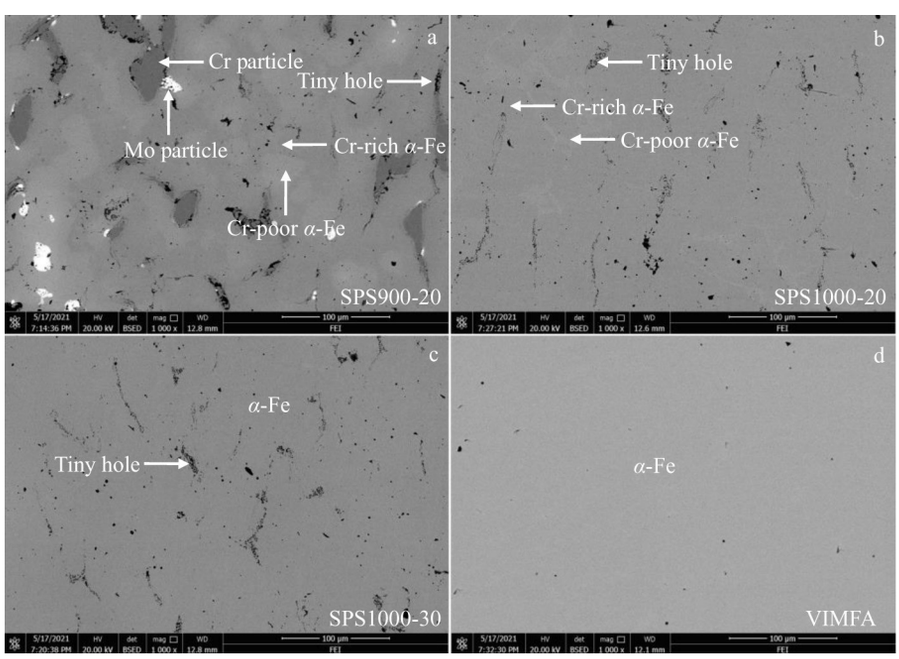

Fig.1 BSE images of Fe-Cr-Mo damping alloys: (a) SPS900-20, (b) SPS1000-20, (c) SPS1000-30, and (d) VIMFA

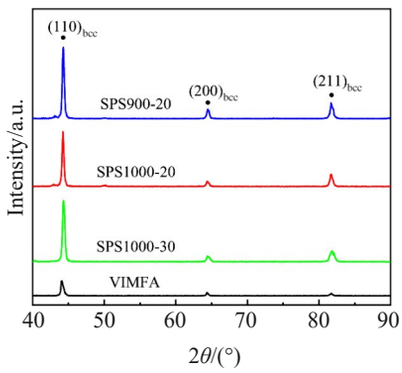

Fig.2 XRD patterns of Fe-Cr-Mo damping alloys

Table 1 Chemical compositions of constituent phases in Fe-Cr-Mo damping alloys determined by EDS in Fig.1 (at%)

Alloy	Phase	Fe	Cr	Mo
SPS900-20	Cr-rich α-Fe	79.98	18.02	2.00
	Cr-poor α-Fe	96.98	1.25	1.77
	Cr particle	0.16	99.84	-
	Mo particle	2.83	0.13	97.04
SPS1000-20	Cr-rich α-Fe	82.01	17.83	1.16
	Cr-poor α-Fe	93.45	5.24	1.31
SPS1000-30	α-Fe	81.61	17.10	1.29
VIMFA	α-Fe	80.92	17.82	1.26

extending the holding time. In addition, some tiny holes are observed in SPS alloys; in spite of this, they still have relatively high compactness (about 97.1%, 98.0% and 98.4% for SPS900-20, SPS1000-20 and SPS1000-30 alloys, respectively). Fig.3 shows the OM microstructures of SPS and VIMFA alloys. It can be seen that the average grains size of SPS alloy slightly rises with increase in sintering temperature, but it is obviously lower than that in VIMFA alloy (about 28, 42, 45 and 320 μm in SPS900-20, SPS1000-20, SPS1000-30 and VIMFA alloys, respectively).

As mentioned above, the SPS900-20 and SPS1000-20 alloys contain gray Cr-rich and light gray Cr-poor α-Fe solid solution. Moreover, it can also be seen from Fig.1a that the Cr particles are primarily surrounded by gray Cr-rich instead of light gray Cr-poor α-Fe solid solution. There are gradually decreased Cr concentrations in Cr particle, Cr-rich and Cr-poor α-Fe phases, successively. Combined with the results regarding variation of area fractions of these phases, it is concluded that the sintering process of SPS alloys, especially the microstructural formation and homogenization, is mainly dominated by the diffusion of Cr elements into α-Fe solid solution. Furthermore, the sintering temperature has a greater influence on the microstructure of SPS alloys than holding time.

2.2 Magnetic performance of Fe-Cr-Mo alloys

Fig. 4 and Fig. 5 show the magnetization curves and hysteresis loops of the alloys under SPS and VIMFA conditions, respectively. It can be seen that the saturation magnetization of SPS alloys is approximate but slightly lower than that of VIMFA one. According to the local magnification details of the hysteresis loops, the SPS alloys have relatively higher coercivity than VIMFA ones (Fig. 5). Generally, the ferromagnetic damping alloy contains many magnetic domains with different magnetic moment directions. These magnetic moments deflect towards the direction of the external magnetic field applied on the alloy and gradually tend to the same direction with increase in intensity of external magnetic field, i. e. saturation magnetization is achieved, accompanied with the irreversible movement of the magnetic

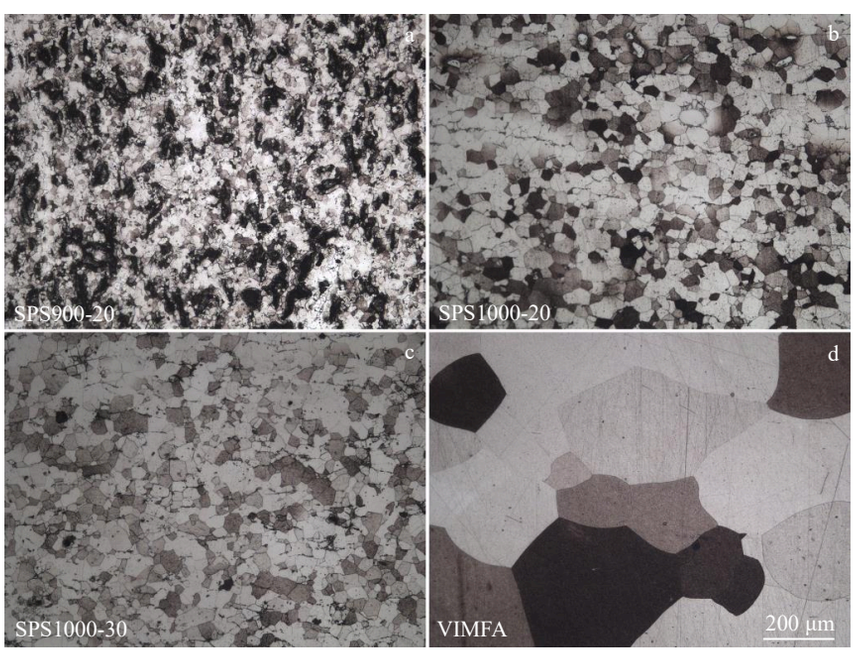

Fig.3 OM microstructures of Fe-Cr-Mo damping alloys: (a) SPS900-20, (b) SPS1000-20, (c) SPS1000-30, and (d) VIMFA

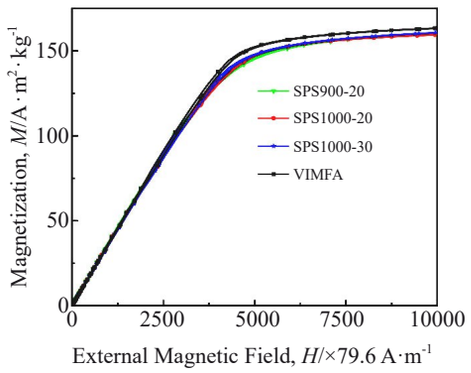

Fig.4 Magnetization curves of Fe-Cr-Mo damping alloys

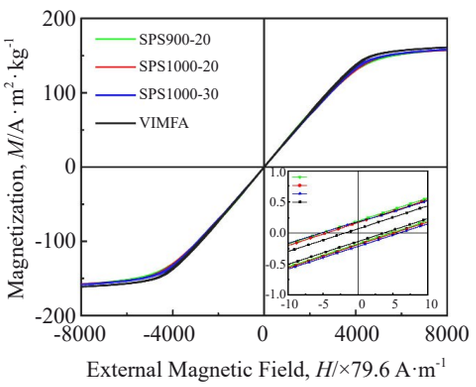

Fig.5 Hysteresis loops and local magnification details of Fe-Cr-Mo damping alloys

domain wall. It is easy to imagine that the deflection of magnetic moment and movement of the magnetic domain wall are bound to be blocked by grain boundaries around, and the obstruction effect is enhanced in SPS alloys with smaller grain sizes and more grain boundaries compared to VIMFA alloys. This illustrates the lower saturation magnetization and higher coercivity in SPS alloys than in VIMFA one to some extent.

2.3 Damping capacity of Fe-Cr-Mo alloys

Fig. 6 shows the variation of the damping capacity of SPS and VIMFA alloys with strain amplitude. As can be seen, all the alloys have relatively high damping capacity and exhibit a tendency of increasing firstly and then decreasing with strain amplitude, and the maximum value appears at strain amplitude of 800×10^{-6} – 900×10^{-6}. The damping capacity of SPS alloy slightly rises with increase in sintering temperature and extension in holding time, although it is still relatively lower than that of VIMFA alloy over the whole strain amplitude range (Fig.6).

It is well known that the damping capacity of the ferromagnetic damping alloys is mainly achieved by the irreversible movement of the magnetic domain wall. According to Ref. [12], the magnetic domain wall will not move across the grain boundary. This is because of the obvious stress concentration at grain boundary so there are very high energy barriers to overcome for movement of magnetic domain wall based on S-B model[13]. The presence of

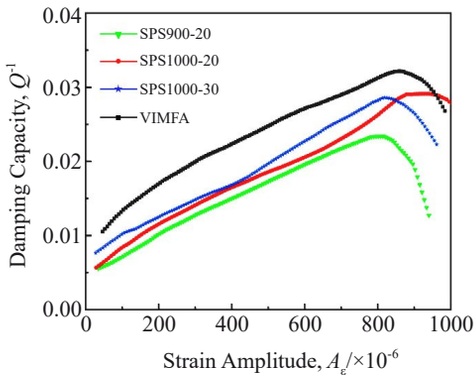

Fig.6 Variation of damping capacity of Fe-Cr-Mo damping alloys with strain amplitude

grain boundary also limits the range of movement of the magnetic domain wall, thus resulting in magnetic hardening of the alloys[14]. The more grain boundaries there are, the higher the energy barriers to overcome and the smaller the range for the movement of the domain walls will be. Therefore it can be deduced that the smaller grain sizes will bring an adverse effect on damping capacity of Fe-Cr-Mo alloys. In addition, the uneven and discontinuous microstructures of SPS alloys, especially when sintered at relatively lower temperature, may hinder the formation of magnetic domain and cause the generation of internal stress, thus resulting in decreased damping capacity. All those mentioned above illustrates the variation of damping capacity of SPS and VIMFA alloys to some extent in this work (Fig. 6), which can also be demonstrated by the results regarding the variation of saturation magnetization and coercivity (Fig.4 and Fig.5).

2.4 Mechanical properties of Fe-Cr-Mo alloys

Fig. 7 shows the compression stress-strain curves of SPS and VIMFA alloys. It can be seen that the compression stress of all the alloys increases rapidly first, then slowly, and eventually generally stable. The compression strength of SPS alloy corresponding to the maximum value of compression stress, rises with increase in sintering temperature, which is higher than that of VIMFA alloy (about 634, 682, 676 and 610

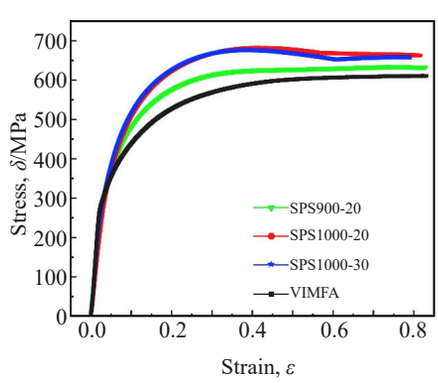

Fig.7 Engineering stress-strain curves of Fe-Cr-Mo damping alloys upon compressing at room temperature with a strain rate of 0.005 s^{-1}

MPa for SPS900-20, SPS1000-20, SPS1000-30 and VIMFA alloys, respectively). As mentioned above, the dissolution of Cr and Mo elements is obviously promoted and the homogeneity of microstructure of SPS alloy is improved by increasing the sintering temperature. Therefore, the better compression property can be obtained by solid solution strengthening effect in the alloys sintered at higher temperatures. The VIMFA alloy has significantly larger grain sizes than SPS one, thus leading to the deceased mechanical property based on Hall-Petch relationship.

3 Conclusions

1) The SPS alloys have high compactness (97.1%−98.4%). With increasing the sintering temperature, the dissolution of elements Cr, Mo etc in α -Fe phase is promoted and the homogeneity of microstructure is obviously improved. The grain size of SPS alloy slightly rises with increase in sintering temperature, while it is obviously smaller than that of VIMA alloy. The sintering process of SPS alloy is primarily controlled by diffusion of Cr and Mo into α-Fe phase.

2) The SPS alloys have lower saturation magnetization but higher coercivity than VIMFA ones. There is favorable damping capacity for SPS alloys despite it is lower than that for VIMFA alloy, and it slightly rises with increase in sintering temperature and extension in holding time. The compression strength of SPS alloys is dramatically higher than that of VIMFA ones, and rises with increase in sintering temperature.

References

1 Hu X F, Li X Y , Zhang B *et al*. *Material Science and Engineering B-Advanced Functional Solid-State Materials*[J], 2010, 171(1–3): 40

2 Wang Hui, Wang Fu, Liu Haitao *et al*. *Material Science and Engineering A-Structure Materials Microstructure and Processing*[J], 2016, 667: 326

3 Xu Xiaoqiang, Xu Yonggang. *Journal of Alloys and Compounds*[J], 2021, 852: 156 673

4 Xu Yonggang, Li Ning, Wen Yuhua. *Journal of Magnetism and Magnetic Materials*[J], 2011, 323(6): 819

5 Xu Yonggang, Li Ning, Wen Yuhua *et al*. *Journal of Alloys and Compounds*[J], 2012, 539: 36

6 Li Xuejun, Liu Ying, Ye Jinwen *et al*. *Rare Metal Materials and Engineering*[J], 2021, 50(7): 2273

7 Dong Duo, Su Yongjun, Zhu Dongdong *et al*. *Rare Metal Materials and Engineering*[J], 2019, 48(12): 4101

8 Ru Jinming, Wang Yuemei, Ruan Hongyan *et al*. *Rare Metal Materials and Engineering*[J], 2020, 49(3): 1075

9 Azcoitia C, Karimi A. *Journal of Alloys and Compounds*[J], 2000, 310(1–2): 160

10 Duan Lian, Pan Dong, Wang Hui. *Journal of Alloys and Compounds*[J], 2017, 695: 1547

11 Karimi A, Azcoitia C, Degauque J. *Journal of Magnetism and Magnetic Materials*[J], 2000, 215: 601

12 Hu X F, Liu X Y, Zhang B. *Materials Science and Engineering A-Structure Materials Microstructure and Processing*[J], 2011, 528(16–17): 5491

13 Smith G W, Birchak J R. *Journal of Applied Physics*[J], 1969, 40(13): 5174

14 Wang Hui, Wang Fu, Xiao Jun *et al*. *Material Science and Engineering A-Structure Materials Microstructure and Processing*[J], 2016, 650: 382

一种放电等离子烧结法制备铁磁型阻尼合金的组织与性能

王舒一，孙美琪，张　松，胥永刚

(西南交通大学 材料科学与工程学院 材料先进技术教育部重点实验室，四川 成都 610031)

摘　要：分别采用放电等离子烧结（SPS）及传统的感应熔炼+锻造+退火（VIMFA）的方法制备了成分为Fe-16Cr-2.5Mo （质量分数，%）的铁磁型阻尼合金。对比研究了SPS和VIMFA合金的组织与性能。结果表明，SPS合金具有较高的致密性。随着烧结温度的增加和保温时间的延长，Cr和Mo元素在α-Fe固溶体中的溶解度明显提高，组织均匀性得到显著改善。与VIMFA合金相比，SPS合金具有相对较低的饱和磁化强度和相对较高的矫顽力。但SPS合金仍然拥有优良的阻尼性能，且随着烧结温度的升高和保温时间的延长，其阻尼能力逐渐增加。SPS合金比VIMFA合金拥有明显提高的抗压缩强度，且随着烧结温度的升高呈现出逐渐增加的趋势。

关键词：Fe-Cr基阻尼合金；放电等离子烧结；磁性能；阻尼性能；力学性能

作者简介：王舒一，男，1999年生，硕士生，西南交通大学材料科学与工程学院，四川 成都 610031，E-mail：1244849964@qq.com